Novel design of integrated thermal functional garment for primary dysmenorrhea relief: The study and customizable application development of thermal conductive woven fabric

Yuanfang Zhao and Li Li*

Institute of Textiles and Clothing, The Hong Kong Polytechnic University, Hong Kong

*Corresponding Author:

Li Li, The Institute of Textiles and Clothing, The Hong Kong Polytechnic University, Hunghom, Kowloon, Hong Kong. Email: li.lilly@polyu.edu.hk

Novel design of integrated thermal functional garment for primary dysmenorrhea relief: The study and customizable application development of thermal conductive woven fabric

Abstract

Thermal garments applied with thermal woven technology especially targeted to relieve primary dysmenorrhea (PD) can hardly be found in the current commercial market. This study had successfully designed, fabricated and studied seven types of thermal conductive woven fabrics woven with two different kinds of silver-coated conductive yarns in three structures, three weft densities and three weft conductive yarn design arrangements, thereby developing a customizable application–an integrated thermal functional garment for PD relief. Appearance, mass, thickness, air permeability, water vapour permeability, thermal conductivity, maximum heat flux, electrical resistance, heating temperature and power efficiency were evaluated to guide the development of an application prototype. On the basis of the results, an optimized design and fabrication were conducted to create a practical and customizable thermal functional garment for PD with successful relief, which can be well industrialized and fill in the commercial gap in the future.

Keywords

thermal conductive woven fabric, thermal functional garment, integrated textile design, primary dysmenorrhea relief

Introduction

Dysmenorrhea refers to the occurrence of painful cramps during women's menstruation.[1] It is a common disease in obstetrics and gynecology and has a great impact on the physical and mental health of female compatriots, which has attracted extensive attention from scholars worldwide. Primary dysmenorrhea (PD) refers to the dysmenorrhea pain not caused by organic disease or specific abnormality in the reproductive organs, for which the incidence rate is highest in adolescent females. Secondary dysmenorrhea is usually caused by pelvic organic lesions such as adenomyosis, endometriosis, pelvic inflammatory disease or cervical stenosis, which are more common in women of childbearing age.[1–3] PD occurs when prostaglandins, a

hormone-like substance produced by uterine tissue, causes intense muscle contraction in the uterus during menstruation. The pain is convulsive and strongest on the lower abdomen, but can also radiate to the back and interior of the thigh. Cramps are usually accompanied by one or more systemic symptoms including nausea and vomiting (89% of women suffering from PD vomited when cramps occurred), fatigue (85%), diarrhea (60%), back pain (60%) and headache (45%). Usually, the symptoms last for hours or one day and seldom last more than two or three days.[2]

Studies indicate that the PD rate is highest among adolescents and young adults and declines with age.[1] Related survey results claim that, for instance, in the United States, 67% of teenagers and 27% of women in their thirties suffered from PD.[1] In Sweden, as high as 90% of adolescents stated PD suffering.[1] In Turkey, the incidence of PD in young women is around 72%,[4] while in China the rate is around 68%.[5] Although there is no organic abnormality in PD, the incidence rate is very high among young unmarried women. The clinical symptoms are obvious, and bring much physical pain and psychological torture to these women, thus greatly reducing their quality of life. In addition, PD becomes the main reason for short-term absenteeism and also causes economic loss. Among adolescent American girls, PD is the leading cause of absence. In the workplace, dysmenorrhea causes 600 million missing work hours in the United States with an economic loss of $2 billion each year.[1]

However, there is currently no specific cure for PD. The methods of treatment and pain relief include non-steroidal anti-inflammatory drugs (NSAIDs), oral contraceptives, surgery, herbal therapy, acupuncture therapy, thermal compression therapy, transcutaneous electrical nerve stimulation and physical exercise.[1,2,6–10] Warming the abdomen or waist area is a well-known non-pharmacological treatment for dysmenorrhea. According to the survey, 75% of young people and more than 50% of teenagers use non-pharmacological methods such as hot water baths and heating pads to relieve the pain of menstruation.[11,12] For instance, in China, 64% of female college students choose hot compresses, while only 18% choose NSAIDs to reduce the painful symptoms.[13] One study has shown that by attaching a piece of heat-and-steam-generating sheet around 38.5°C to the skin of the lower abdomen for 8 h, 57% and 63% of the subjects felt relief of abdominal pain, and 54% and 61% of the

subjects felt relief of low back pain on the first and second day of menstruation, respectively. The results prove that the application of a heating pad can be used as a non-pharmacological method to alleviate the symptoms of PD.[10]

The current commercial market provides a hot water bag or hot patch for women to use for dysmenorrhea. A thermal garment is one kind of heating clothing that provides warmth. However, the existing thermal jacket only targets the chest, back, waist, leg or foot, and the thermal pad is either knitted with conductive yarn or produced by non-woven carbon fibers. When searching on the internet, there are plenty of brands of heated garments displayed on Amazon, eBay and AliExpress.[14–16] Even famous brands such as warmX, Ravean and AVADE only have the above mentioned products.[17–19]Limited commercial thermal garments especially targeted for dysmenorrhea have been developed, not to mention products applying thermal conductive woven fabrics (TCWFs). There are abundant researches of thermal conductive knitted fabrics and apparels in studying the resistance models, fabric performance and functional garment development.[20–24] There are several researches about resistance models of TCWF;[25,26] however, limited research has been generated in fabric performance and functional garment development of TCWF.

In this study, novel TCWFs are designed and fabricated. After studying and optimizing the TCWFs, an integrated commercial-oriented thermal functional garment is designed and developed by adopting the optimized design combination. This thermal garment can operate as a thermal therapy treatment apparel when suffering PD, and can be worn as a normal attractive clothing in the spare time as well. The thermal woven technology will not limit the design. On the contrary, it can coordinate with pattern design and outfit design to meet even unique requirements. In addition, this thermal garment can target different body parts with different temperatures by calculation and weaving arrangement. The manufacturing process only takes one-step formation. In addition, the garment adopting this TCWF is soft, light and customizable, and is totally different from the thermal jacket in the current market. Last, the design method of TCWF development, apparel development and supporting accessory development effectively reduces the material waste, energy consumption and financial cost. The integrated thermal functional garment for PD

relief can be a positive sample and experience for further commercial garment development, which is likely to become the future inspiration and guidance of industrial design and production.

TCWF design

The TCWF sample is designed with dimensions of 12 cm (4.8 in) in width and 15 cm (5.9 in) in length (Figure 1(a)). Plain weave, twill weave (1/3) and satin weave (8 ends) are used for structural changes (Figure 1(b) to (d)). Weft densities are 25 picks/in, 30 picks/in and 35 picks/in, respectively, while warp density maintains 40 ends/in. As demonstrated in Figure 1, silver-coated conductive yarn A (SCCY A) is designed to weave in every weft pick, in every other weft pick and in every five weft picks. Silver-coated conductive yarn B (SCCY B) is designed to be placed in the warp direction using it as a conductive path due to its electrical resistance, which is much higher than the electrical resistance of SCCY A. The area between the two conductive paths is the heating area which provides thermal treatment. The heat is generated by the electrical current through every SCCY A as resistors. Figure 2lists the design specifications of all seven TCWF experiment samples: P25-S1, P25-S2, P25-S6, P30-S6, P35-S6, T25-S2 and S25-S2. The letters P, T and S stand for the structure of plain weave, twill weave and satin weave, respectively. The numerals 25, 30 and 35 represent the weft densities. The labels S1, S2 and S6 denote the SCCY A design arrangement. In the structure images, a mark in a square indicates that the end is over the pick at the corresponding place in the fabric, i.e. warp up. A blank square indicates that the pick is over the end, i.e. weft up. The green square represents SCCY A and the black square represents basic yarn.
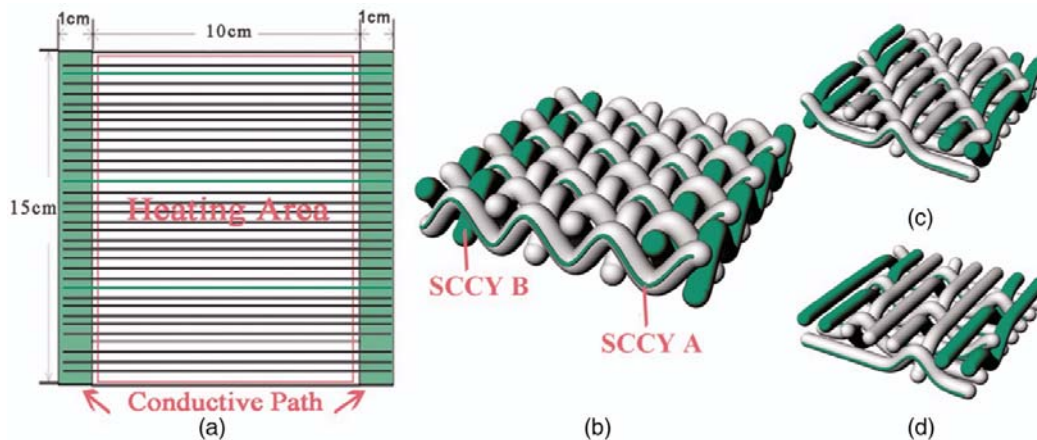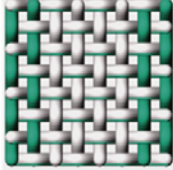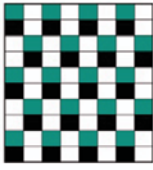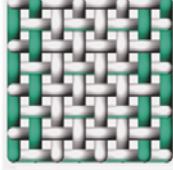

(a) (b) (c) (d)
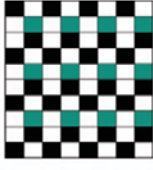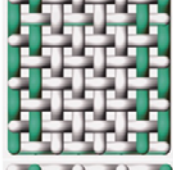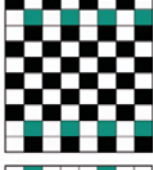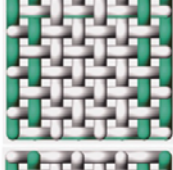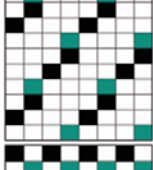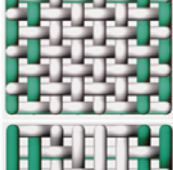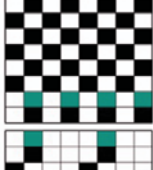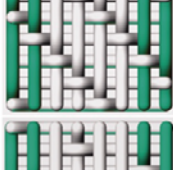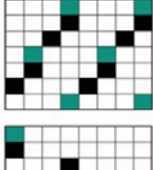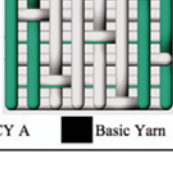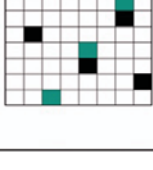
Figure 1. Thermal conductive woven fabric design description: (a) size and function of sample; (b) plain weave and illustration of SCCY A and SCCY B; (c) twill weave; (d) satin weave.

SCCY: silver-coated conductive yarn.

Fabric Code	3D Image	Structure Image	Fabric Structure	Fabric Density		SCCY A Design Arrangement
				Weft (picks/inch)	Warp (ends/inch)	
P25-S1			Plain Weave	25	40	Every Pick (+0)
P25-S2			Plain Weave	25	40	Every Other Pick (+1)
P25-S6			Plain Weave	25	40	Every Five Picks (+5)
P30-S6			Plain Weave	30	40	Every Five Picks (+5)
P35-S6			Plain Weave	35	40	Every Five Picks (+5)
T25-S2			Twill Weave (1/3)	25	40	Every Other Pick (+1)
S25-S2			Satin Weave (8 ends)	25	40	Every Other Pick (+1)

Note: ▮ SCCY A ▮ Basic Yarn

Figure 2. Specifications of the thermal conductive woven fabric sample design.

SCCY: silver-coated conductive yarn.

Experiment

Material

100% cotton Ne 20/2 yarn was used as the basic yarn in both the weft and warp directions. The two yarns SCCY A and SCCY B were used as electrical conductive materials. SCCY A was woven in the weft direction while SCCY B was placed in the warp direction. The microscope images and yarn specifications are listed in Figure 3.

Label	a	b	c
Material	100% Cotton	Silver-coated Nylon 6	Silver-coated Nylon 66
Yarn Count	Ne 20/2 S ply	22/1 dtex single filament	235/34 dtex 2-ply
Diameter	0.308 mm	0.005 mm	0.290 mm
Electrical Resistance	N/A	72.6 Ω/cm	1.1 Ω/cm
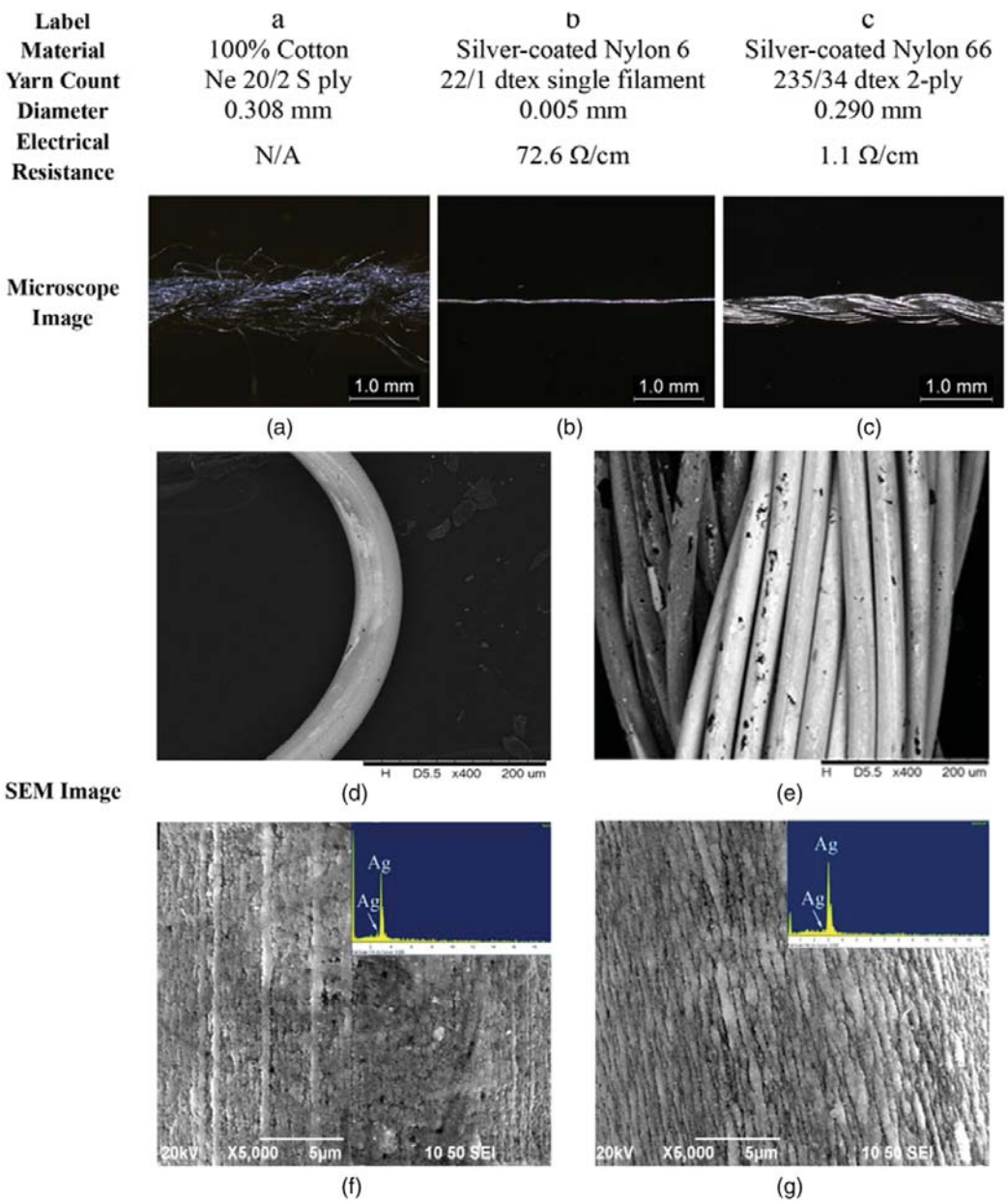
Figure 3. Yarn specifications and images of material used: (a) microscope image of cotton yarn; (b) microscope image of SCCY A; (c) microscope image of SCCY B; (d) SEM image of SCCY A; (e)

SEM image of SCCY B; (f) SEM image with EDS image of SCCY A; (g) SEM image with EDS image of SCCY B.

EDS: energy dispersive spectroscopy; SCCY: silver-coated conductive yarn; SEM: scanning electron microscopy.

Fabrication

The TCWF samples designed in this experiment were woven by a CCI automatic dobby sampling loom (CCI Tech Inc.) as shown in Figure 4(a), (b) and (d). Density trial and structure trial were conducted as well in Figure 4(a) and (b). The head type is gripper head with speed of around 25 rpm. As displayed in Figure 4(c), six groups of 1-cm cotton warp yarns were replaced by the SCCY B. In order to accomplish this replacement, a small warp beam was produced by only SCCY B, and additionally attached behind the original cotton warp beam. In case of deformation and poor quality in the edge area, it is necessary to place the replaced region in the middle of the warp yarns. As shown in Figure 4(d), the right group in the green box was too close to the right edge, which led to the unstable quality of this group of samples. Enough samples were fabricated and qualified samples were selected for this study. The fabrics in the selvedge areas have not affected the test results in this study. Since the yarn strengths are fully different, the cotton yarn is easily broken during weaving. When continuing, the tension of the yarn is changed thus affecting the fabric density. This is because the limitation of this sampling loom is that the yarn strength cannot be maintained. Only by reweaving the sample can successful samples be obtained, as shown in Figure 4(a). Therefore, the rejection rate of the sample is relatively high. By changing to a professional weaving loom, the rejection rate would be low. Figure 4(e) shows the weaving design of the weft yarn of all samples. The change of order of "X" means to shift and to weave a different pick. SCCY A is woven with one basic yarn without shift for stabilizing the position of this yarn.
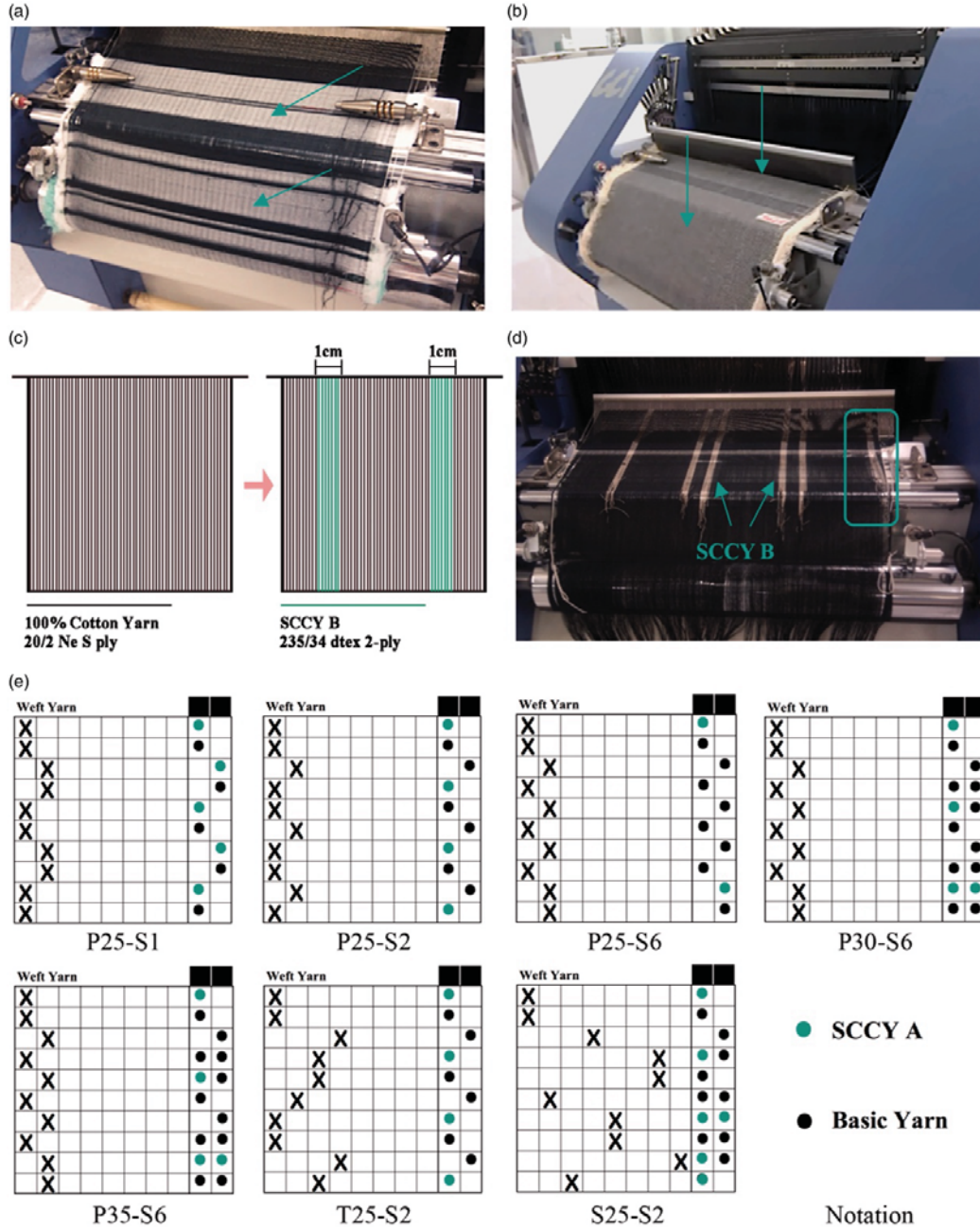
Figure 4. Fabrication experiment: (a) weft density weaving trial; (b) structure weaving trial; (c) warp yarn replacement design; (d) warp yarn replacement effect; (e) weft yarn weaving design. SCCY: silver-coated conductive yarn.

Basic test

All samples were tested in a control room under the KSON control system with an air pressure of 1 atm, relative humidity of $65 \pm 2\%$, and temperature of $23 \pm 1°C$. For measurement purposes, all samples were placed inside the control room for 24 h

before testing and none of them were treated with washing or ironing before testing. The testing samples and times are listed in Table 1.

Advantages	Works in the future

✓ PD period - thermal therapy treatment apparel
  Other time - a normal attractive clothing
	→ Wear trial
	  - PD treatment effect test
	  - Thermal comfort test

✓ Coordinate with pattern design and outfit design	

✓ Target at different body parts with different temperatures
  by calculation and weaving arrangement
	→ Laundry test
	  - Waterproof process

✓ One-step formation	→ Drying test - Anti-oxidation process
✓ Soft, light and customizable	

✓ Reduce the material waste, energy
  consumption and financial cost
	→ Corrosion test
	  - Anti-NaCl process

✓ Positive sample and experience for further commercial garment development	→ Electrical safety test → Market survey
✓ Future inspiration and guidance of industrial design and production	→ Commercialization → New product development

PD: primary dysmenorrhea.

Test	Mass test	Thickness test	Air permeability test	Water vapour permeability test	Thermal conductivity test	Qmax test	Electrical resistance test	Heating temperature test
Number of testing times	5	5	10	3	5	5	5	3

Table 1. Testing sample quantity and testing times

Mass and thickness test

The mass of the samples was tested by the AY210 electronic balance equipment with a readability of 0.1 mg, and the thickness of the fabrics was tested under the pressure 392.266 Pa by the RMES equipment. Each sample was measured five times and the average value was calculated.

Air permeability test

The air permeability was evaluated on a KES-F8-AP1 air permeability tester according to standard ASTM D 737. The sample was placed on the circular testing head. This test was carried out under an air velocity of 0.02 m/s. Air resistance of each sample was measured at 10 random points and the average value was calculated.

Water vapour permeability test

The water vapour permeability was measured according to GB/T 12704.1-2009. The moisture permeable cup, containing a desiccant and the fabric sample, was placed in a sealed environment of certain temperature and humidity mentioned previously. The

water vapour permeability was calculated according to the change of the fabric mass and environment pressure after 24 h.

Thermal conductivity and maximum heat flux test

The KES-F7 Precise and Fast Thermal Property-Measuring Instrument Thermo Labo II was used to test the thermal conductivity. The sample was placed onto the testing area of the instrument, and the heat loss values and maximum heat flux (Q_{max}) values were measured. The test for each type of sample was repeated five times. The thermal conductivity (k) value was calculated according to the equation:

$$k = W \cdot d/a \cdot \Delta T$$

(1)

where W is heat loss (in Watts), d is thickness (in millimetres), a is tested area (25 cm^2) and ΔT is temperature difference (10°C).

Electrical resistance test

The sample was aligned on an insulated hard board and its electrical resistance was measured by a four-probe method with a Keithley 2010 multimeter. Each sample was measured five times and the average value was calculated.

Heating temperature test

The sample was aligned on an insulated hard board and was heated by the Daxin DX3005DS digital control direct current power supply under certain voltage. The fabric temperature was measured by the Functional Material Innovation Limited temperature sensor. Five temperature sensors were placed evenly on the surface of the sample to measure the temperature. The temperature range is around and temperature precision is . The humidity range is 0–100% relative humidity and humidity precision is . Thermal images were taken by the FLIR E33 thermal imaging camera.

Results and discussion

Appearance

In total, seven types of TCWF samples were produced and three samples of each were selected under the same parameters. Sample images and microscope images are displayed in Figure 5. The conductive paths in the warp direction were well fabricated among all structures. In the weft direction, SCCY A presents a different status when

structure and density change. This is because when decreasing the density or changing the structure to twill weave or satin weave, limited tensile force caused by more float yarns and less overlaps were acted on SCCY A. In its natural state, SCCY A is wave-shaped rather than straight-shaped. So, as weft density increased, the skewness of the fabric is more obvious.
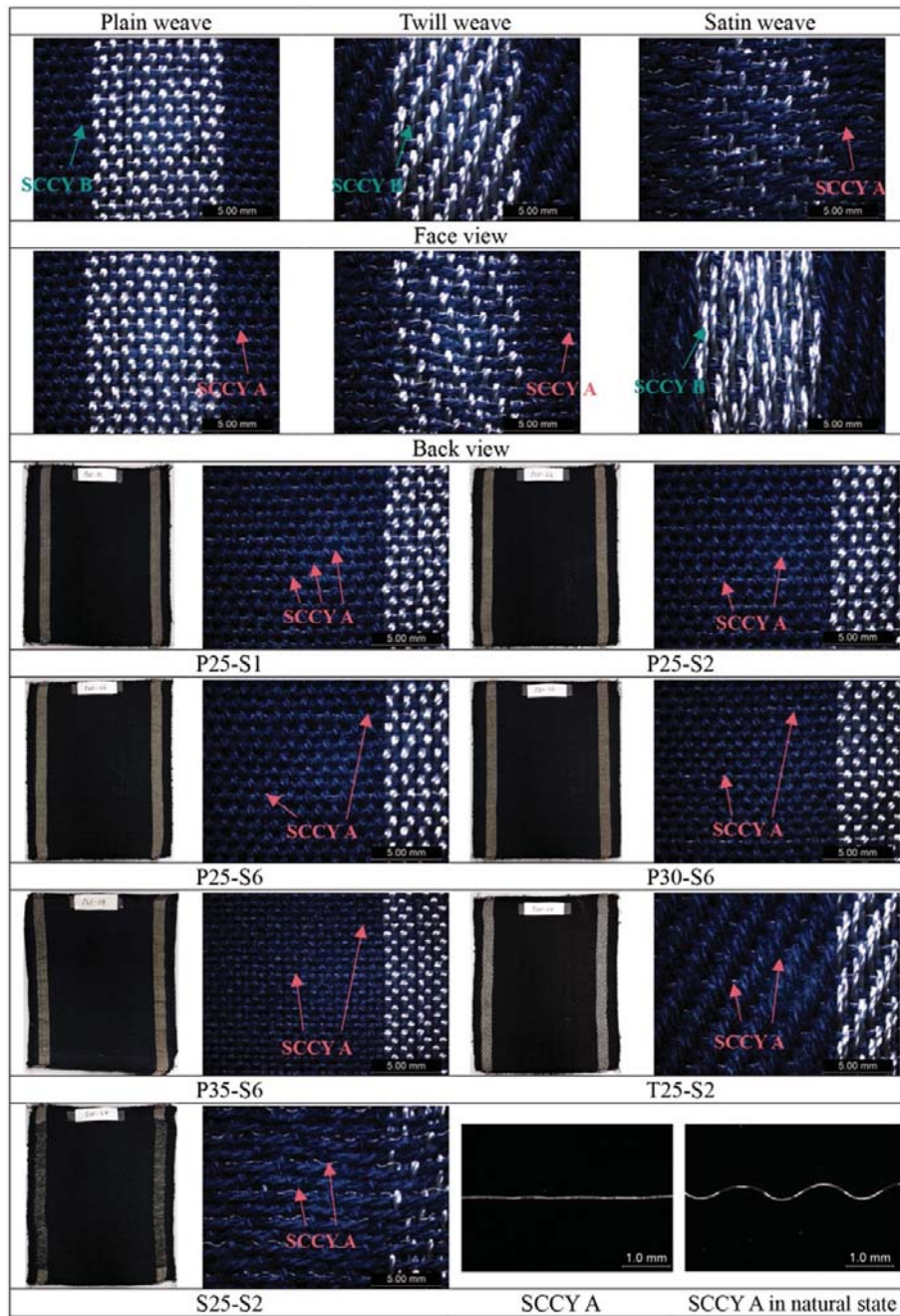
Figure 5. Thermal conductive woven fabric samples and microscope images.

SCCY: silver-coated conductive yarn.

Mass and thickness

Figure 6(A) shows the results of sample mass and thickness. When the weft density and structure remained unchanged, the sample mass was slightly decreased as SCCY A design arrangement decreased (less SCCY A were woven into the fabric). The number of SCCY A yarns woven in the weft direction can obviously influence the mass. When the structure and SCCY A design arrangement stayed the same, the mass increased apparently as the weft density increased. The increase in weft density visibly added sample mass. When the weft density and SCCY A design arrangement remained the same, the mass increased when the structure changed from plain weave to twill weave and satin weave. The structure became loose when changing from plain weave to satin weave, as there were more yarns existing at the same per unit area, thus augmenting the mass. In terms of sample thickness, it followed the same tendency. The thickness almost remained the same when SCCY A design arrangement decreased while the weft density and structure stayed unchanged. The adjustment of the number of SCCY A barely changed sample thickness. The thickness increased when the weft density was raised while the structure and SCCY A design arrangement remained the same. More yarns existed in the same per unit area, which affected the thickness in an apparent way. The thickness was noticeably increased when the structure changed from plain weave to satin weave while the weft density and SCCY A design arrangement remained unchanged. Satin weave is a looser structure with less pressure between the yarns than twill weave, which keeps more yarn curves that result in a greater thickness. Twill weave is similar to plain weave. All sample masses are less than 200 g/m^2 and around 167 g/m^2 in average, which are normal fabric masses that can be used in common garment making. All sample thicknesses are lower than 1.1 mm and around 0.75 mm in average, which are much lighter than existing products.

A - Test results of sample mass and thickness							
Sample	**P25-S1**	**P25-S2**	**P25-S6**	**P30-S6**	**P35-S6**	**T25-S2**	**S25-S2**
Weight (g/m²)	160	159	156	182	192	162	163
Mass (mm)	0.65	0.64	0.64	0.67	0.71	0.87	1.06

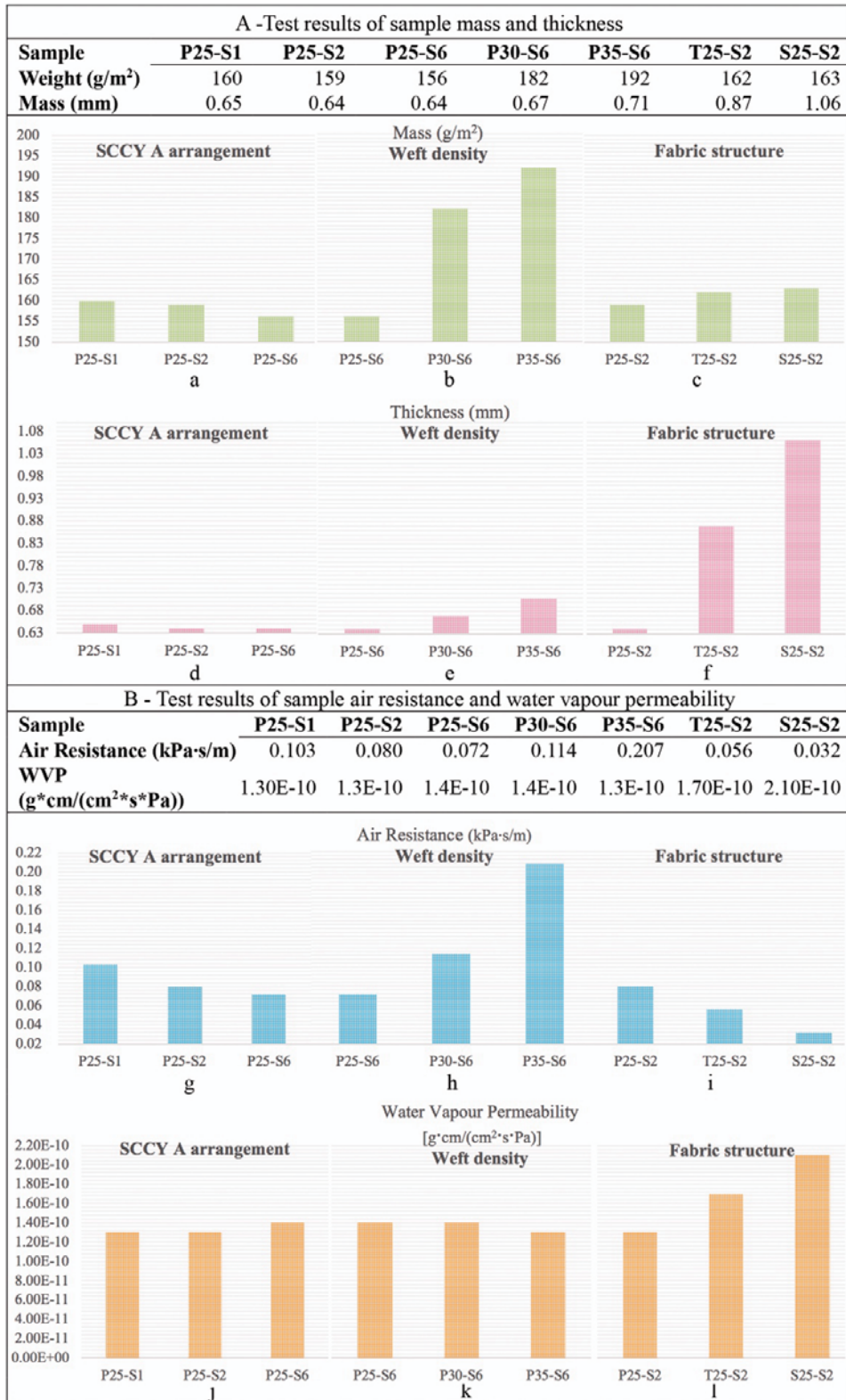| B - Test results of sample air resistance and water vapour permeability							
Sample	**P25-S1**	**P25-S2**	**P25-S6**	**P30-S6**	**P35-S6**	**T25-S2**	**S25-S2**
Air Resistance (kPa·s/m)	0.103	0.080	0.072	0.114	0.207	0.056	0.032
WVP (g*cm/(cm²*s*Pa))	1.30E-10	1.3E-10	1.4E-10	1.4E-10	1.3E-10	1.70E-10	2.10E-10

Figure 6. Test results of sample mass, thickness, air resistance and water vapour permeability.

SCCY: silver-coated conductive yarn; WVP: water vapour permeability.

Air permeability

Air resistances of all samples were measured and the results are shown in Figure 6(B). The smaller the value of air resistance, the better the air permeability of the sample. According to the results, the air permeability of all samples was less than 0.12 kPa·s/m and 0.09 kPa·s/m on average, which represents good air permeability. When SCCY A design arrangements decreased, the air resistance decreased, which means the air permeability enhanced as the SCCY A lessened. The decrease in SCCY A provided the space for air to flow. In the same per unit area, the increase in weft density reduced the hollow space for air, which evidently raised the air resistance. As weft density increased, the air permeability dropped sharply. When the fabric structure changed from plain weave to satin weave, the air resistance lessened. As the structure became looser, more hollow spaces developed, which led to better air permeability.

Water vapour permeability

Water vapour permeability can to some extent present the thermal comfort property of fabric. The key influence factor of moisture vapour permeability is the condition of the moisture transfer channel. Currently, there are three major kinds of channels. The first one is when the gaseous water directly diffuses through the pores between the yarns in the fabric and the pores between the fibers in the yarn. The second one is when the gaseous water condenses into a liquid on the inner surface of the fabric through the inter-fiber pores and the intra-fiber pores in the yarn. The water is transported by capillary action to the outer layer of the fabric and then evaporates into gaseous water to diffuse into the outer space. The third one is when liquid water is transported to the outer layer of the fabric through the inter-yarn pores and inter-fiber pores in the fabric and then evaporates into gaseous water to diffuse into the outer space. The water vapour permeability of the fabric is actually a comprehensive reflection of these three channels of water vapour permeability.

All the test results are listed in Figure 6(B). The greater the value of water vapour permeability, the better the water vapour transportation property of the sample. According to the results, when SCCY A design arrangements decreased, the water vapour permeability increased, which means the water vapour transportation property

enhanced as the amount of SCCY A was reduced. As more cotton yarn replaces SCCY A yarn, the moisture wicking ability of the fabric will be improved. As weft density increased, the water vapour permeability decreased. The hollow space between warp yarn and weft yarn can absorb and lock moisture or water. The higher density causes fewer hollow spaces thus weakening the water vapour transportation property of the fabric. Since the structure became much looser when changing from plain weave to satin weave, more hollow spaces developed, which led to much better vapour transportation.

Thermal conductivity and Q_{max}

Thermal conductivity results of k values are listed in Figure 7(A). A higher k value reflects a better thermal conductivity that heat is more easily transferred. When the structure and weft density are maintained, the thermal conductivity slightly decreases when SCCY A design arrangement decreases. The reduction of conductive yarn marginally degrades the thermal conductivity. When the structure and SCCY A design arrangement stayed the same, the k value increased apparently as weft density increased. As weft density increased, longer conductive yarns are woven into the fabric which increases the thermal conductivity. When the weft density and SCCY A design arrangement remained unchanged, the k value varied when the fabric structure changed from plain weave to satin weave. Apparently, a looser structure enhances the thermal conductivity due to more hollow spaces being added, such as twill structure compared with plain structure. However, when the structure is over loose, the heat dissipation rate is fast so that the heat transfer ability decreases, such as satin structure compared with twill structure. Thermal conductivity of the TCWF sample has some relation with conductive material woven in but significant relation with fabric structure.

A - Test results of sample thermal conductivity (k) and Qmax							
Sample	**P25-S1**	**P25-S2**	**P25-S6**	**P30-S6**	**P35-S6**	**T25-S2**	**S25-S2**
k ($W·m^{-1}·K^{-1}$)	0.0610	0.0576	0.0572	0.0633	0.0709	0.0582	0.0541
Qmax ($W·cm^{-2}$)	0.106	0.097	0.090	0.109	0.111	0.088	0.084

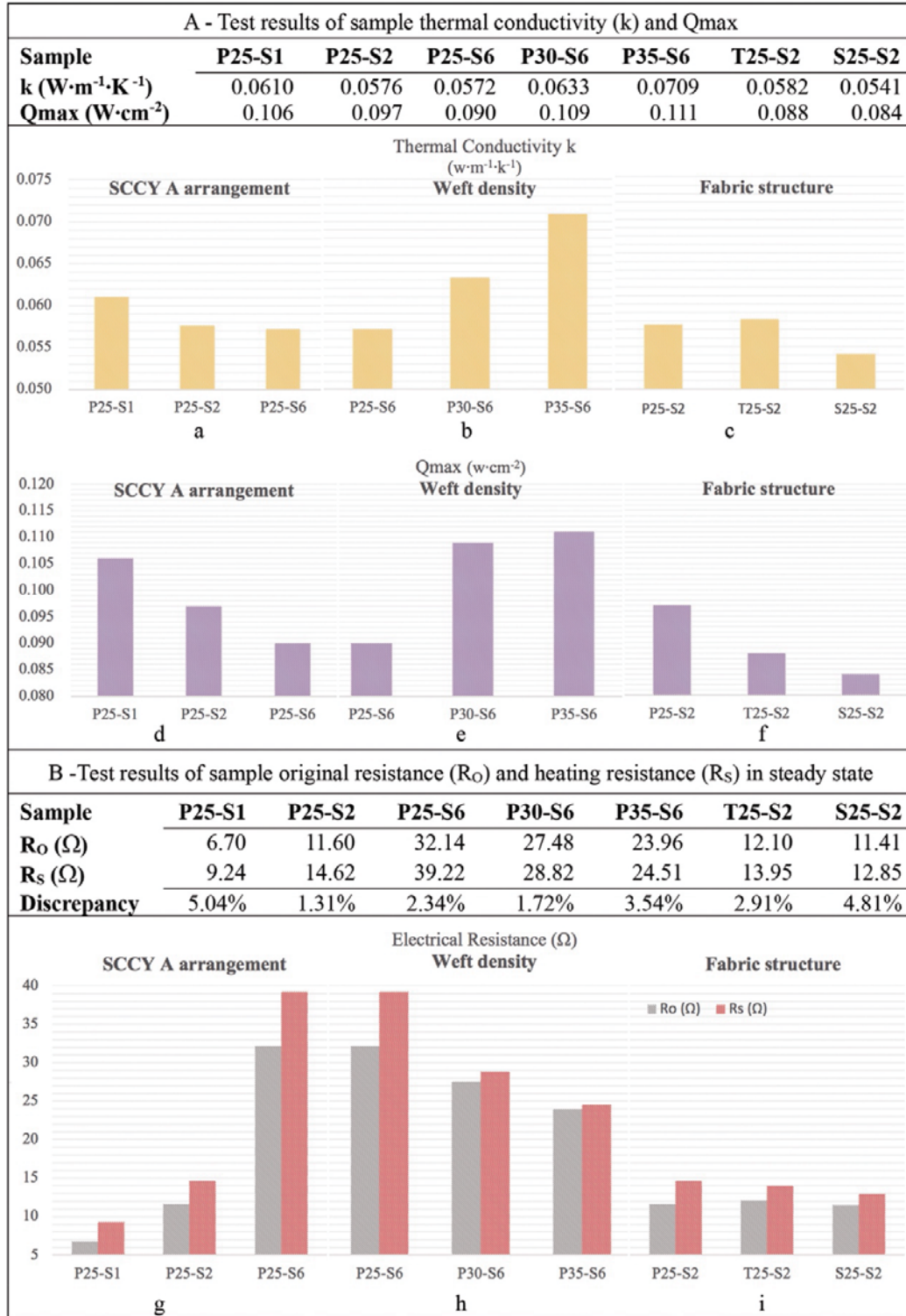| B -Test results of sample original resistance (R_O) and heating resistance (R_S) in steady state							
Sample	**P25-S1**	**P25-S2**	**P25-S6**	**P30-S6**	**P35-S6**	**T25-S2**	**S25-S2**
R_O (Ω)	6.70	11.60	32.14	27.48	23.96	12.10	11.41
R_S (Ω)	9.24	14.62	39.22	28.82	24.51	13.95	12.85
Discrepancy	5.04%	1.31%	2.34%	1.72%	3.54%	2.91%	4.81%

Figure 7. Test results of sample thermal conductivity (k), Q_{max}, sample original resistance (R_O) and heating resistance (R_S) in steady state.

Qmax: maximum heat flux; SCCY: silver-coated conductive yarn.

Qmax values (i.e. peak heat fluxes that can reflect the warm/cool feeling evaluation) are listed in Figure 7(A). A lower Q_{max} value represents a slow heat dissipation rate, which provides a warmer feeling. When SCCY A design arrangement decreased, the Q_{max} value decreased, which means the fabric is warmer as the conductive yarn lessened. When the weft density increased, the Qmax value boosted, which means more conductive yarns woven into the fabric lead to a cooler feeling. When the fabric structure changed, the Qmax value diminished, which means the satin structure has a warmer feeling than the twill structure mostly due to the hollow space increased by the structure. Air is a poor conductor of heat; therefore, if a large amount of still air stays in the hollow space, it leads to a better warmth.

Electrical resistance

Electrical resistance before heating (R_o) and after heating in steady state (after 20 min heating) (R_s) were measured and are listed in Figure 7(B). When only SCCY A design arrangement parameter decreased, fabric resistance enormously enlarged. Since weft conductive yarns were woven into the fabric in parallel, the smaller the quantity, the higher the electrical resistance. When only the weft density parameter increased, the fabric resistance decreased. The increase in weft density increased the length of SCCY A used, which increased the single yarn resistance but decreased the fabric resistance due to the parallel connection. When only the fabric structure parameter changed, the electrical resistance had a minor difference. Theoretically, the different structure may cause different resistance since the tightness will impact the length of conductive yarn woven into the fabric, which will affect the whole fabric resistance. However, in this experiment, the combination of weft density of 25 picks/in and SCCY A arranged every other pick may not obviously reflect the difference caused by structure. Further experiments will be conducted to look into this issue. According to Joule's law:

$$Q = I^2 Rt$$

(2)

where Q (in Watts) is the amount of heat generated, I (in Amperes) is the electric current flowing through a conductor (heating area of TCWF sample), R is the electrical resistance of the TCWF sample, and t is the time the electrical current is flowing. The electrical resistance is the major determining parameter for thermal performance when the power supply settled (voltage unchanged). The smaller R is, the

more heat Q will be generated. Therefore, the TCWF sample with a smaller R value has more heat, and thus has a higher thermal temperature effect than those with a larger R value.

However, when the temperature is not constant during heating the resistance value of conductive yarn varies, as shown in Figure 8. The heating temperature increased gradually on heating and tended to be stable after 20 min. However, this heating temperature would influence R in return. Normally, a linear approximation of electrical resistivity of metals is used for evaluating the percentage change in resistance value:

$$\rho(T) = \rho_0 \left[1 + \alpha \cdot (T - T_0)\right]$$

(3)

where ρ is the electrical resistivity of the conductor material (silver), ρ_0 is the

electrical resistivity of silver at T_0, α indicates the temperature coefficient of

resistivity of silver at T_0, and T_0 is a fixed reference temperature (usually room

temperature). As demonstrated in the images of Figure 8, the electrical resistance sharply increased in the first 2 min and slightly decreased until 5 min and almost remained the same until heating to 20 min. This may be because in the first 2 min, the fabric temperature rapidly rose and the electrons absorbed more energy and moved faster, which led to more scattering, thus increasing the amount of resistance. After 2 min, the temperature started slowly increasing while the conductive yarn expanded the length, surface and volume, which may all have led to a reduction of fabric resistance. From 5–20 min, the temperature tended to be steady and the conductive yarns were expanded to their maximum, thus the fabric resistance had a slight change during this period. When SCCY A changed, the expansion of the R value was marginally increased. When the weft density increased and the fabric structure changed, the expansion of the R value was reduced. The discrepancy between R_S and R_O was around 3.04%.

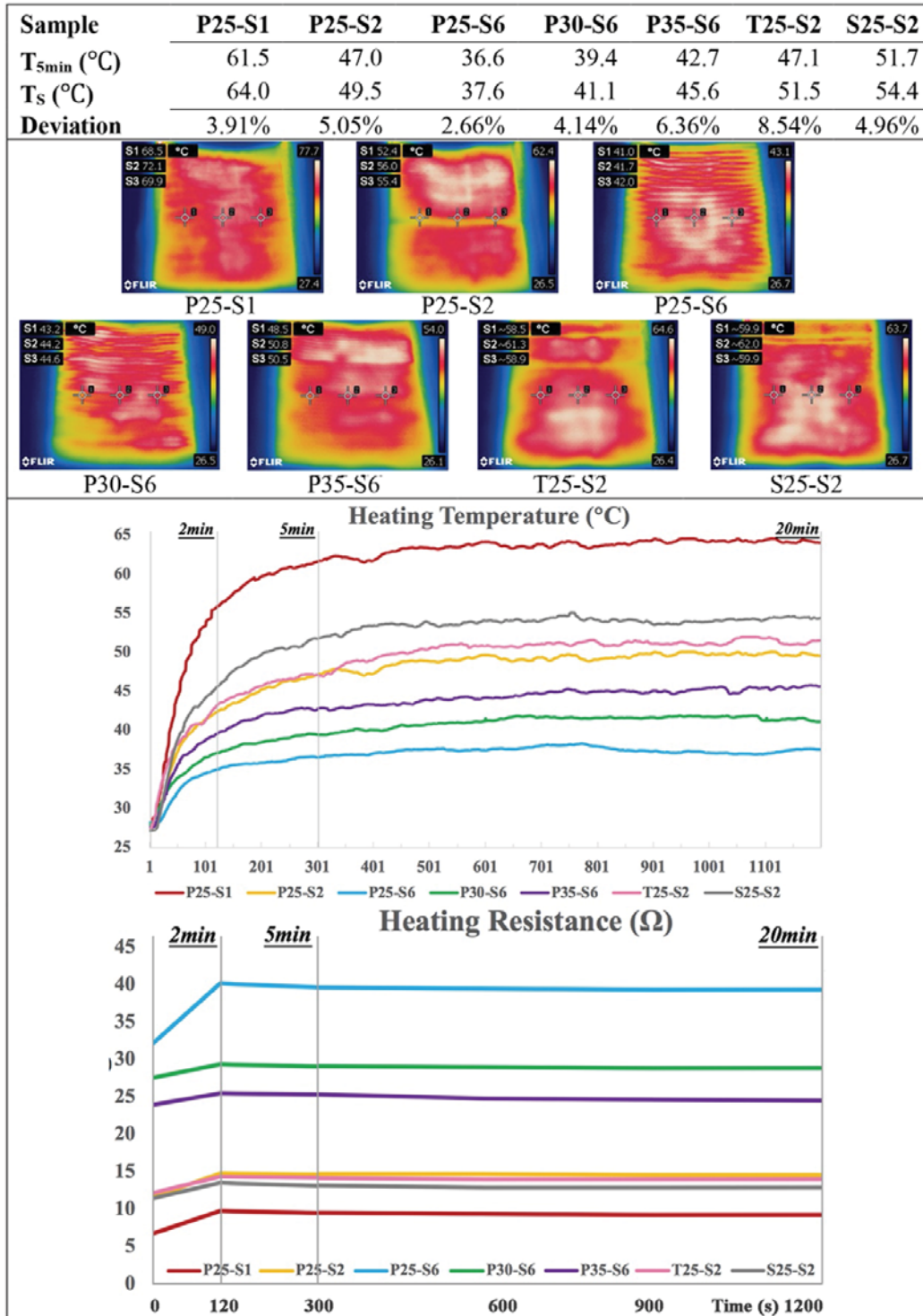| Sample	P25-S1	P25-S2	P25-S6	P30-S6	P35-S6	T25-S2	S25-S2
T_{5min} (°C)	61.5	47.0	36.6	39.4	42.7	47.1	51.7
T_s (°C)	64.0	49.5	37.6	41.1	45.6	51.5	54.4
Deviation	3.91%	5.05%	2.66%	4.14%	6.36%	8.54%	4.96%

Figure 8. Test results of sample heating temperature and heating resistance.

Temperature

All samples were heated by a power supply under 10V and the results are shown in Figure 8. During the first 2 min, the heating temperature rose rapidly and gradually

increased until 5 min. Then the heating temperature slowly increased and almost maintained a certain temperature until 20 min which were defined as steady state. The infrared images in Figure 8 show the thermal effect at steady state. The deviations between $T_{5\,min}$ and T_S was around 5.02%, which meant that in the first 5 min of heating, the TCWF samples were almost reaching maximum temperature which may to some extent represent the fabric temperature in an approximate way. As illustrated in the images of Figure 8, the testing results presented similar results according to Joule's law in the previous section: a lower resistance generated more heat. When SCCY A was the only independent variable, the heating temperature dropped due to the increase of resistance caused when the amount of SCCY A was reduced. When the weft density was the independent variable, the temperature rose due to the increase in resistance triggered by densification of the weft density. However, although some samples had similar resistance, the steady temperatures were different. The P25-S2, T25-S2 and S25-S2 had similar electrical resistance with the same weft density and SCCY A design arrangement but different fabric structure. On heating, the discrepancy in the temperature effects was greater compared with the resistance difference. Due to the lower thermal conductivity and lower Qmax, the heat was much harder to be transferred and had a lower dissipation rate in the satin weave compared with the twill weave. Therefore, the steady temperature of S25-S2 was higher than T25-S2. However, the twill weave had a higher thermal conductivity but lower Qmax compared with the plain weave, which led to the slightly higher temperature. This is a quite interesting phenomenon; it indicates that when designing a substitute sample, the structure and other weaving parameters which affect the target temperature will need to be seriously considered. In addition, a customized temperature requirement can be realized by the structure and other weaving parameter designing, which will have a potential business market.

However, the silver-coated yarn has its limitations. As demonstrated in Figure 3, the microscope images and scanning electron microscopy images of SCCY A and SCCY B, the silver-coated particle is not as stable as the pure metal yarn. It has the possibility of exfoliation and oxidation, which may cause a change in electrical resistance, thus causing an uneven thermal effect to occur. This is the key issue to work on in the future for commercialization. The low temperature can be the

consequence of exfoliation and oxidation. In addition, it may occur since there is a different dissipation on the fabric.

In addition, all the samples were measured by the same temperature sensor and were tested under the same circumstances; therefore, the variations in temperature are under the same error system. This means the relative values between each data are meaningful. Moreover, all the fabrics were measured under the same infrared radiation, and therefore the data values are effective. Furthermore, the previous temperature results were real-time results with certain deviation. However, due to the influence of heat dissipation, to achieve a more accurate temperature would be to consider the impact of complex environment conditions. The deep analysis of this issue will be thoroughly studied in the next phase.

Power

When electrical current flows through a conductive fabric, heat is generated in the embedded conductive yarns. The amount of heat released is proportional to the square of the current multiplied by the electrical resistance of conductive yarn. The formula for heating (in Joules) is

$$P = IU$$

(4)

where P (in Watts) is the power converted from electrical energy to thermal energy, I (in Amperes) is the current flowing through conductive yarns, and U (in Volts) is the current working voltage. Since Ohm's law is applicable here, the formula can be rewritten in the equivalent form

$$P = I^2 R = U^2/R$$

(5)

where R (Ω) is the equivalent resistance of the TCWF samples. In this experiment,

direct current is the only consideration. The temperature of the surface of the TCWF sample rises when a power supply is connected. Heat capacity is the measurable physical quantity that specifies the amount of thermal energy required to change the temperature of an object by a given amount. It is defined as the ratio of the amount of thermal energy Q (in Joules) transferred to an object and the resulting increase in temperature T (in Kelvin) of the object:

$$C = Q/\Delta T \tag{6}$$

Normally, the term specific heat capacity C (joule/kilogram·kelvin) which is defined as heat capacity per unit mass is more commonly used for experimental and theoretical purposes. Ideally, all the thermal energy transferred from electrical energy will be absorbed by the fabric in a given time duration t (second). Therefore, we can deduce

$$Pt = Q = cm\,\Delta T \tag{7}$$

where m (in kilograms) is the mass of the TCWF sample. However, in practice, there will be a certain amount of heat loss to the surrounding environment. A quantity $\eta(\%)$ is thus introduced which refers to the percentage of thermal energy contributing to the increase in temperature of the conductive fabric. Thus, the equation will be

$$Pt\,\eta = cm\,\Delta T \tag{8}$$

or

$$(U^2/R)t\eta = cm\,\Delta T \tag{9}$$

Thus, the amount of increase in temperature is approximately proportional to the square of the voltage applied to the TCWF sample.

In this experiment, the electric power P is not constant since the resistance value R is temperature dependent. Therefore, transient analysis has to be conducted to study the detailed heating process. The model of heat transfer can be described as

$$Q = W + S \tag{10}$$

where Q is the electrical energy provided to the fabric, W is the actual energy absorbed by the fabric contributing to the temperature rising, and S is the energy dissipated to the surrounding environment. Assuming a very short time interval, it has

$$dQ = dW + dS \tag{11}$$

where it is known that

$$dQ = P \cdot dt \tag{12}$$

$$dW = cm \cdot dT \tag{13}$$

$$dS = \alpha(T - T_0) \cdot dt \tag{14}$$

where α is the heat dissipation coefficient (W/K) calculated in Figure 9. The energy transmission equation is

$$T = (P/\alpha) \cdot \left(1 - e^{-\alpha t/cm}\right) + T_0 \tag{15}$$

when $t=\infty$, approaching steady state temperature Ts, which gives the steady-state equation

$$T_S - T_0 = P/\alpha = U^2/\alpha R(U) \tag{16}$$

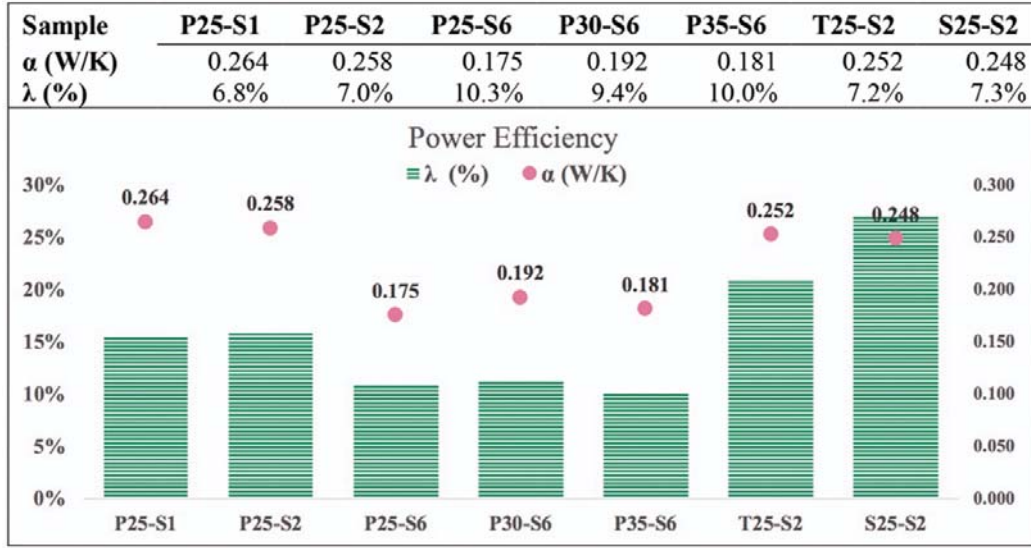| Sample	P25-S1	P25-S2	P25-S6	P30-S6	P35-S6	T25-S2	S25-S2
α (W/K)	0.264	0.258	0.175	0.192	0.181	0.252	0.248
λ (%)	6.8%	7.0%	10.3%	9.4%	10.0%	7.2%	7.3%

Figure 9. Results of sample power utilization efficiency.

In steady state, the heat transfer reaches equilibrium point at which $dW=0$, that is $dQ=dS$ at $T=Ts$ at ; the equation

$$P \cdot dt = \alpha(T - T_0) \cdot dt \tag{17}$$

gives the same result. From the above equations, we could find that the rate of increase in temperature depends on the heat dissipation coefficient, the specific heat capacity, and the mass of TCWF fabric. A high rate of heating requires a larger α, and smaller c and m. The final temperature depends on the electric power P and the heat dissipation coefficient α. This indicates the final temperature could be manually designed using different materials, fabric structure, densities and voltage.

In order to compare the power utilization efficiency, λ was calculated to demonstrate the results, as shown in Figure 9. According to Fourier's law,

$$Q = -kA(dT/dx) \cdot dt \tag{18}$$

where k (W·m−1·K−1) is the thermal conductivity, A (m²) is the surface

area, T (Kelvin) is the surface temperature and x is the coordinate point on the surface. When reaching the steady state,

$$\lambda = S/Q \tag{19}$$

where

$$Q = (k/d)A(T_S - T_0) \cdot dt \tag{20}$$

and

$$S = I^2 R \cdot dt = P \cdot dt \tag{21}$$

where d (in metres) is the fabric thickness. Thus,

$$\lambda = dI^2 R / kA(T_S - T_0) \tag{22}$$

As illustrated in Figure 9, the heat dissipation coefficient has some association with power utilization efficiency. When SCCY A was the only independent variable, both α value and λ value decreased due to the decline of heat generation source caused when the amount of SCCY A was reduced. When weft density was the independent variable, both α value and λ value were almost the same since the heat generation source remained unchanged. Moreover, if the structure is too loose or too tight, the power utilization efficiency will also be affected. When fabric structure was the independent variable, the power efficiency was sharply enhanced while the heat dissipation coefficient slightly decreased. This indicated that the extra-gained space in the structure to a large extent influenced the power efficiency and improved the thermal effect.

Application development of integrated thermal functional garment for PD relief

Garment design

The apparel application, a one-piece dress, is designed with a modern chic style and targeted for the autumn–winter season. Digital printing with a Chinese ink style is used on the outer fabric. The lining is one-step formation woven with the TCWF structure. The lining fabric will provide the warmth when connecting the detachable battery controller. The heating panel is designed as 15 cm in length and 20 cm in width and is located in the abdomen area. The width of the conductive path is 1cm. The concept of this thermal functional garment is that when switching on the controller, the dress can heat to the appropriate temperature which will relieve the pain caused by PD. When not in menstruation, the battery controller can be detached, then the whole dress becomes a normal charming dress. Unlike the heated garment in the current market, this dress has an aesthetic outlook and thermal functionality simultaneously. All detailed specifications are presented in the design sheet in Figure 10.
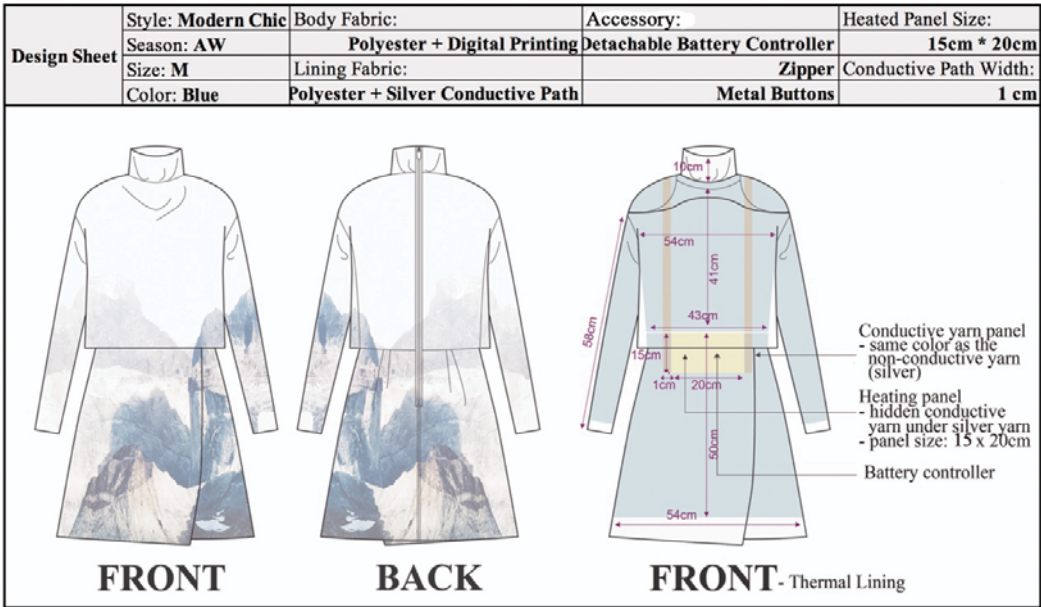

Figure 10. Design sheet of thermal functional garment.

Thermal functional panel development

TCWF design and fabrication

Since the fabric woven by the CCI sampling loom is not suitable for the lining, in the application stage, a professional weaving loom was adopted: the Staubli jacquard loom and Dornier weaving loom (SD loom). Unlike the extra warp beam made for SCCY B when weaving by the CCI loom, it was impossible and unreasonable to

produce a new SCCY B warp beam for the SD loom just for sample making. Therefore, in order to weave the lining sample, the warp yarn replacement became the first step. Two groups of warp yarns were manually replaced by SCCY B for 1 cm each. Combining the previous experiment result of the TCWF design, the SCCY A was woven in the weft direction every pick. Plain weave was applied in both the conductive path and the heating panel. The size of the heating panel was 15 cm in length and 18 cm in width. The actual electrical resistance was 5.1 Ω. Under 7.5 V, the heating temperature at stable status T_s was around 49°C. All the design and fabrication specifications are demonstrated in Figure 11.

Weft yarn	100% Polyester, blue color	Weft density	30 picks/cm (76 picks/in)
Warp yarn	100% Polyester, white color	Warp density	47 ends/cm (119 ends/in)
Sample size	15cm * 20cm	Structure	Plain weave
Heating panel	SCCY A, +0, 15cm * 18cm	Conductive path	SCCY B, 1cm
Electrical resistance	5.1 Ω	Stable Temperature	49 °C

Warp yarn replacement of Staubli jacquard loom and Dornier weaving loom

Weaving notation

● Basic Yarn
● SCCY A

TCWF sample for application   Microscope Image   Thermal Image
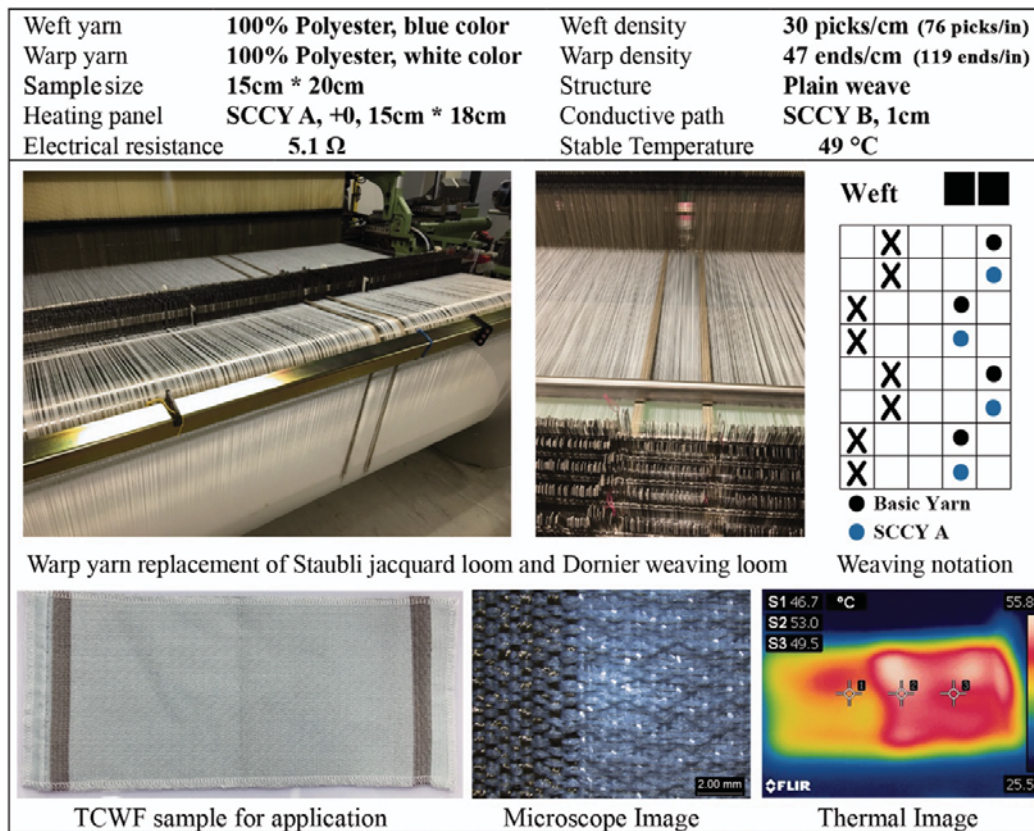
Figure 11. Design and fabrication specifications of the thermal conductive woven fabric sample for apparel application.

SCCY: silver-coated conductive yarn; TCWF: thermal conductive woven fabric.

TCWF optimization

After testing the TCWF sample for apparel application, several modifications were made to optimize the fabric. First, the width of conductive path was widened to 2 cm in order to increase the electrical resistance and lower the current when connecting

power. Second, the SCCY A weaving arrangement was changed from every pick to every five picks for material saving and current reduction. Third, different weaving structures were designed for different areas to achieve better hand feel, aesthetic performance, quality control and safety concern. As shown in Figure 12, the heating area D was fabricated in double layers, thus the SCCY A can be hidden between the outer fabric and the lining to prevent unexpected breaking. Figure 12 thoroughly illustrates the design of the different optimized linings in sections A, B, C, D and E. Sections C, D and E are double layers with different structures in the face and back. On the face of section E, the heating panel can easily be seen by the SCCY A yarn which is responsible for warmth, whereas on the back of section E, the SCCY A yarn is hidden and hard to access. In addition, the irregular weave pattern on the back of section E and the totally different weaves in sections A, B, C and D are specially designed to prove the pattern can be customized without affecting the heating effect. Last, the heating area was enlarged to meet the design requirement. All the design and

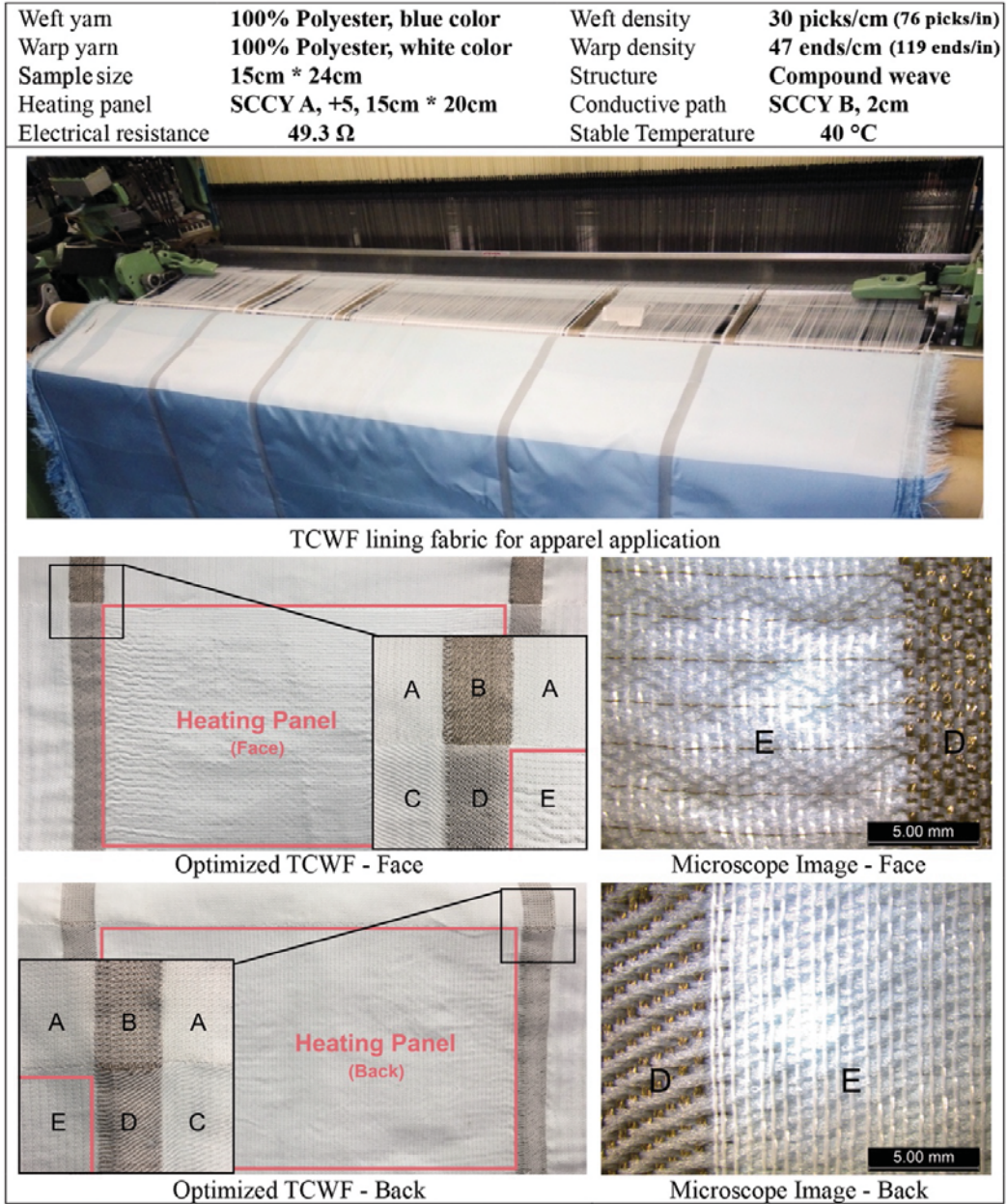fabrication specifications are displayed in Figures 12 and 13.

Weft yarn	**100% Polyester, blue color**	Weft density	**30 picks/cm (76 picks/in)**
Warp yarn	**100% Polyester, white color**	Warp density	**47 ends/cm (119 ends/in)**
Sample size	**15cm * 24cm**	Structure	**Compound weave**
Heating panel	**SCCY A, +5, 15cm * 20cm**	Conductive path	**SCCY B, 2cm**
Electrical resistance	**49.3 Ω**	Stable Temperature	**40 °C**

TCWF lining fabric for apparel application

Optimized TCWF - Face

Microscope Image - Face

Optimized TCWF - Back

Microscope Image - Back

Figure 12. Design and fabrication specifications of optimized thermal conductive woven fabric lining for apparel application.

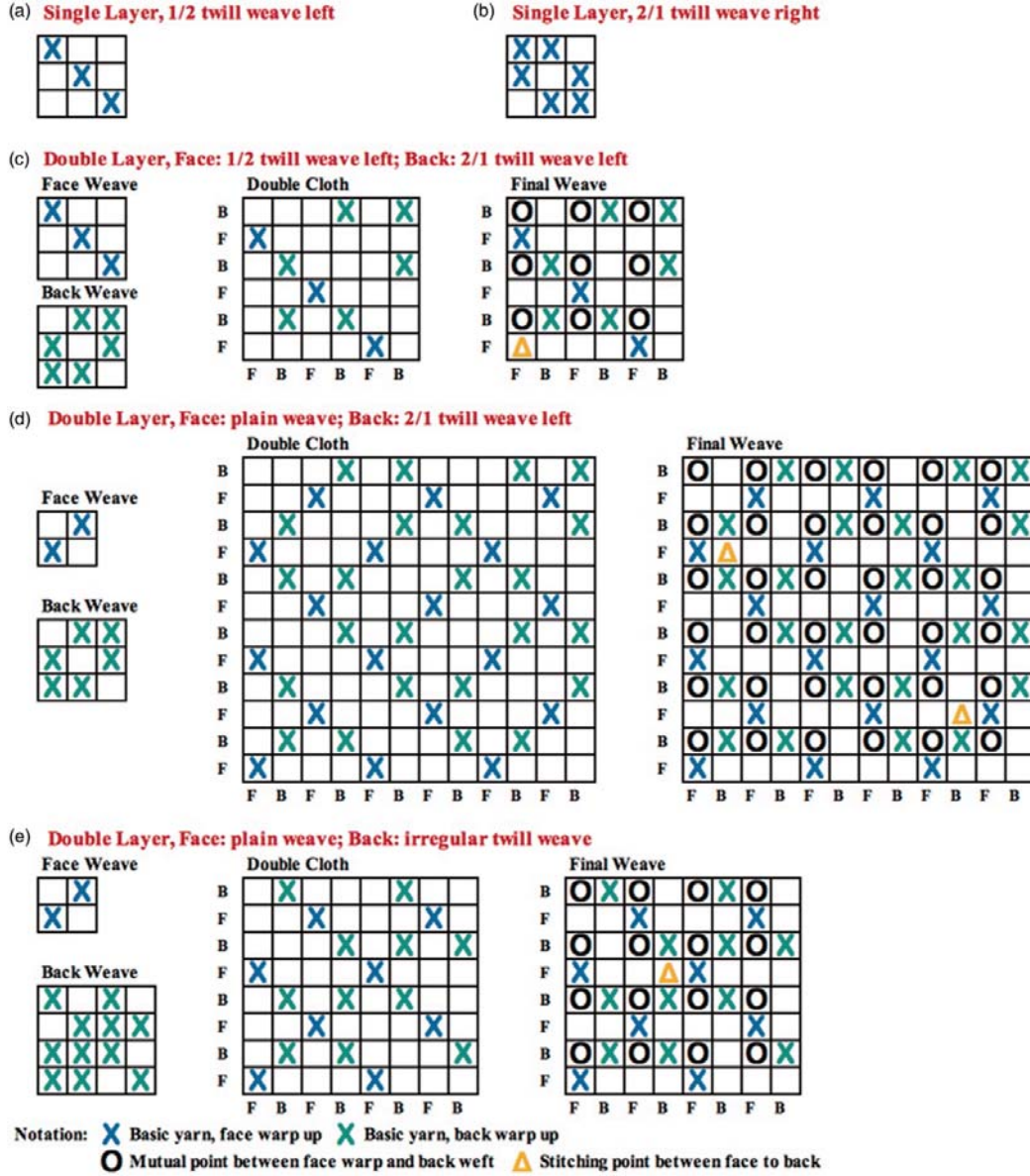SCCY: silver-coated conductive yarn; TCWF: thermal conductive woven fabric.

Figure 13. Notation of weaving design for optimized thermal conductive woven fabric.

Detachable controller development

A detachable controller system is one major element in wearable electronics, of which the control device is mostly the troublesome part to design due to the various limitations in size, output voltage and discharge time in order to reach a suitable and desired condition. The battery size and capacity affect all of the above parameters. In this paper, a detachable controller prototype for performing the thermal functional garment was designed, as show in Figure 14(a) to (d). A practical design was produced to meet the following specifications: (a) safe; (b) attachable; (c)

rechargeable battery; (d) with a similar shape and size to a cell phone; (e) constant heating condition up to 2 h. A charging administrative module for a 7.4 V Li battery, like those in cell phones, was used, which contains the function of protection board, balanced charger and charging process suitable for Li-ion or Li-ion polymer batteries. It is the implementation of digital electronics. So far, the control system is operating mainly as analogue power electronics. A relatively large-sized electronic component is required due to the relatively high power consumption and large current. Although only around 15 W and 1 A, which is quite small in the range of power electronics, compared with digital electronics this could be quite high. The future could be a combination of digital electronics with flexible printed circuit boards. In that case, the size of device could be greatly reduced. However, the technical part is challenging. Currently, the controller was attached by metal buttons onto the electrical path which was specially designed and woven into the fabric. Based on this control system, the thermal functional garment reached the expectation.
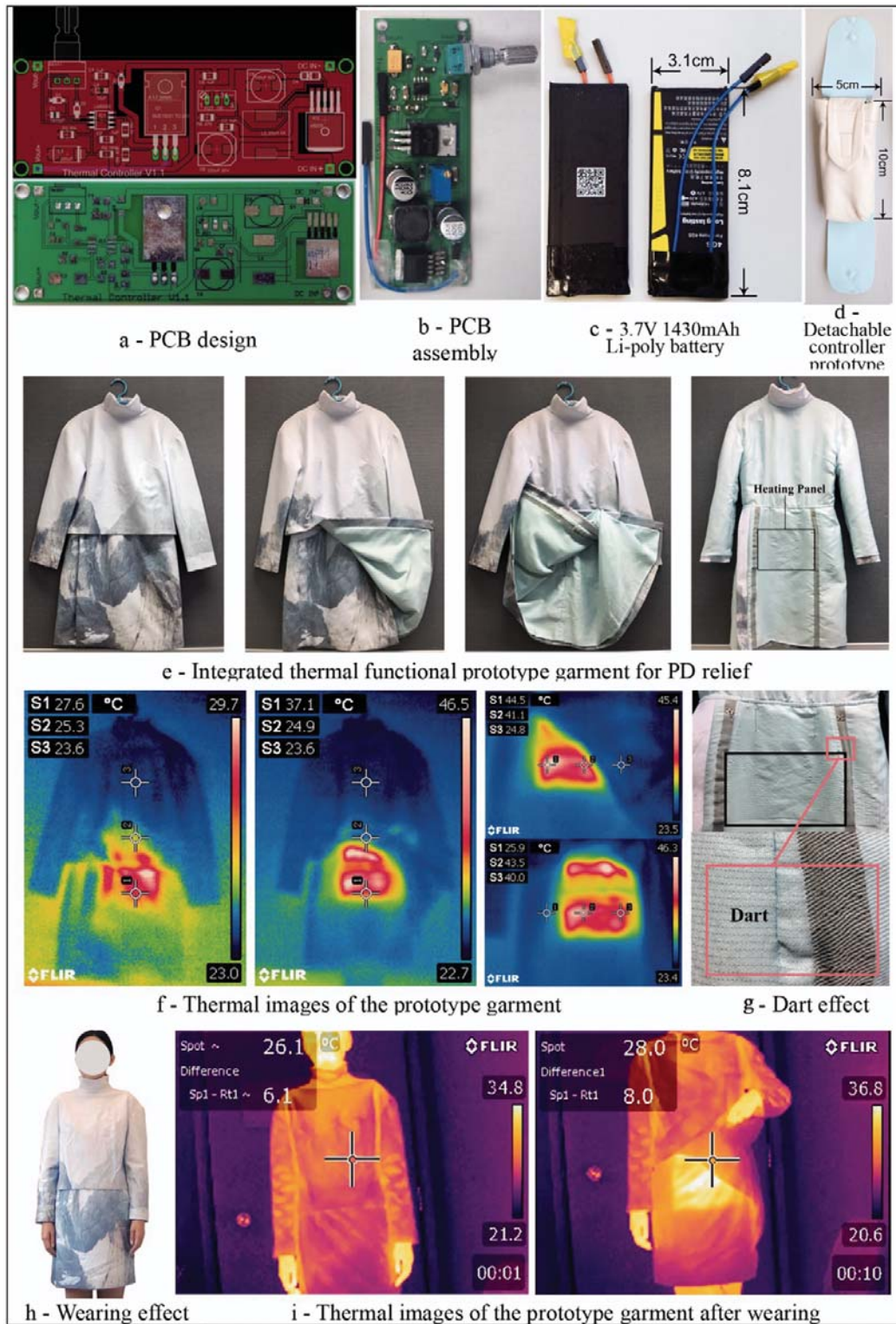
Figure 14. Prototype development of the integrated thermal functional garment for primary dysmenorrhea relief.

PCB: printed circuit board; PD: primary dysmenorrhea.

Apparel application development

An integrated application, as displayed in Figure 14(e), the thermal functional dress for PD relief, was well produced. The outer fabric was digitally printed according to the design pattern and lining was woven based on the optimized TCWF design. The lining can be sewn like normal lining fabric. Even the sewing of darts will not influence the eventual thermal outcome, Figure 14(g). The thermal images in Figure 14(f) present the heating effect when connected to the battery controller. The targeted area worked as designed and reached the temperature as expected.

Wearing effect

We selected one female subject who was approximately 165 cm in height and 60 kg in mass with PD condition to try the dress on (Figure 14(h)). The thermal panel was targeted to her abdomen area. When switching on the controller, the treatment panel immediately warmed up (Figure 14(i)). The thermal images taken by the infrared camera well demonstrated the effect. It reached 38°C within 2 min and stabilized around 20 min at 40°C. After continuously warming for 30 min, the female subject claimed obvious relief from the menstrual pain. In further study, a professional wear trial will be conducted to fully evaluate the effectiveness of the thermal dress for PD relief and thermal comfort, which will guide the industrial design and production for optimization and commercialization.

Future work

The TCWF and the integrated thermal garment adopting this fabric tentatively meet the requirement and realize the initial intention. The advantages are listed in Table 2. These advantages already make the integrated thermal garment competitive in the market. However, in order to accomplish commercialization, a series of important future work needs to be done. First, more vital tests will be conducted. A wear trial is a key test to evaluate the PD treatment effect and the thermal comfort. The data will be the first-hand experience and will guide the modification of the product. A laundry test, drying test and corrosion test will lead to the necessity of a waterproof process, anti-oxidation process and anti-NaCl process. Since the silver-coated yarn in not stable as metal yarn, these processes will play an important role in future commercialization. Another essential test is an electrical safety test. The garment has

to meet the related standard to avoid severe consequences. Ideally, the last part is the preparation for final commercialization. These future works will be delivered in two stages: post-test and modification stage and commercialization preparation stage.

Advantages	Works in the future
✓ PD period - thermal therapy treatment apparel. Other time - a normal attractive clothing	→ Wear trial - PD treatment effect test - Thermal comfort test
✓ Coordinate with pattern design and outfit design	
✓ Target at different body parts with different temperatures by calculation and weaving arrangement	→ Laundry test - Waterproof process
✓ One-step formation	→ Drying test - Anti-oxidation process
✓ Soft, light and customizable	
✓ Reduce the material waste, energy consumption and financial cost	→ Corrosion test - Anti-NaCl process
✓ Positive sample and experience for further commercial garment development	→ Electrical safety test → Market survey
✓ Future inspiration and guidance of industrial design and production	→ Commercialization → New product development

PD: primary dysmenorrhea.

Table 2. Advantages and future work

Conclusion

Seven types of TCWFs, with three structures, three weft densities and three weft conductive yarn design arrangements, woven with two different kinds of silver-coated conductive yarns were designed, fabricated and tested. The results of appearance, mass, thickness, air permeability, water vapour permeability, thermal conductivity, Qmax, electrical resistance, heating temperature and power efficiency can guide the development of application. The structure majorly influenced the fabric thickness, air permeability, water vapour transportation property, thermal effect and power efficiency except electrical resistance. Weft density had a minor effect on thickness and power efficiency whereas it had a considerable influence on air permeability, thermal effect and resistance. SCCY A design arrangement significantly changed thermal effect, resistance and power efficiency. According to the results of the evaluations, optimized design and fabrication were conducted. The width of the conductive path was widened to 2 cm in order to increase the electrical resistance and lower the current when connecting power. The SCCY A weaving arrangement was settled with every five picks for material saving and current reduction. Different weaving structures were designed for different areas to achieve better hand feel, aesthetic performance, quality control and safety concern. The heating area was

fabricated in double layers thus the SCCY A can be hidden between the outer fabric and the lining to prevent unexpected breaking.

The thermal functional garment for PD was practical, customizable and successfully relieved menstrual pain. This garment can operate as a thermal therapy treatment apparel when suffering PD, as well as being worn as a normal attractive clothing at other times. The thermal woven technology can well coordinate with different design requirements, and can target different body parts with different temperatures by calculation, weaving arrangement and one-step formation. The garment adopting this TCWF is soft, light and customizable, which is totally different from the thermal jacket in the current market. The design method of TCWF development, apparel development and supporting accessory development effectively reduces the material waste, energy consumption and financial cost. The integrated thermal functional garment for PD relief can be a positive sample and experience for further commercial garment development, which is likely to become the future inspiration and guidance of industrial design and production.

References
1. Mai T, Odle TG and Frey RJ. *Dysmenorrhea.* Cengage Learning, 2011, pp.1429–1433.
2. Dawood YM. Dysmenorrhea. In: Dadelszen PV (ed) *The global library of women's medicine*. London: GLOWM, 2008.
3. Lee LC, Tu CH, Chen LF, et al. Association of brain-derived neutophic factor gene Val66Met polymorphism with primary dysmenorrhea. *PLOS One* 2014; 9: 1–10.

4. Nivashini G. Prevalence of primary dysmenorrhea along with irregular periods. *Res J Pharm Technol* 2015; 8: 1099–1106. .

5. Sun YM, Wang L, Li G. Investigation on influencing factors of primary dysmenorrhea in 1800 female college students. *Tianjin J Tradit Chin Med* 2009; 5: 367–369.

6. Chen YT, Cao Y, Xie YH, et al. Traditional Chinese medicine for the treatment of primary dysmenorrhea: how do Yuanhu painkillers effectively treat dysmenorrhea?. *Phytomedicine* 2013; 20: 1095–1104.

7. Ji B, Ren XX, Zhao YF, et al. Comments on study of pathogenesy, prevention and treatment of primary dysmenorrhea. *China J Mod Med* 2008; 18: 1856–1862.

8. Davis AR, Westhoff CL. Primary dysmenorrhea in adolescent girls and treatment with oral contraceptives. *J Pediatr Adolesc Gynecol* 2001; 14: 3–8.

9. Wang ZJ, Li KF, Dong GJ, et al. Study on the biological mechanism of exercise training for dysmenorrhea. *Sport* 2015; 119: 153–154. .

10. Hosono T, Takashima Y, Morita Y, et al. Effects of a heat- and steam-generating sheet on relieving symptoms of primary dysmenorrhea in young women. *J Obstet Gynaecol Res* 2010; 36: 818–824.

11. O'Connell K, Davis AR, Westhoff C. Self-treatment patterns among adolescent girls with dysmenorrhea. *J Pediatr Adolesc Gynecol* 2006; 19: 285–289.

12. Campbell MA, McGrath PJ. Non-pharmacologic strategies used by adolescents for the management of menstrual discomfort. *Clin J Pain* 1999; 15: 313–320.

13. Zhang QM. Analysis of influence factors to primary dysmenorrhea of Coedna. *J Hanjiang Univ* 2012; 40: 68–71. .

14. Heated Jacket. https://www.amazon.com/s/ref=nb_sb_noss_1?url=search-alias%3Daps&field-keywords=heated+jacket&rh=i%3Aaps%2Ck%3Aheated+jacket (accessed 6 July 2018).

15. Heated Jacket. https://www.ebay.com/sch/i.html?_from=R40&_trksid=m570.l1313&_nkw=Heated+Jacket&_sacat=0 (accessed 6 July 2018).

16. Heated Jacket. https://www.aliexpress.com/wholesale?catId=0&initiative_id=SB_20180705202523&SearchText=heated+jacket (accessed 6 July 2018).

17. Warming Clothes for Women. https://www.warmx.de/shop/index.php?main_page=index&cPath=1&sort=20a&language=en (accessed 6 July 2018).

18. Heated Jackets. https://ravean.com/pages/heated-jackets (accessed 6 July 2018).

19. Heated Garments. http://www.avade.com.au/products.html (accessed 6 July 2018).

20. Li L, Au WM, Wan KM, et al. A resistive network model for conductive knitting stitches. *Text Res J* 2010; 80: 935–947.

21. Li L, Au WM, Hua T, et al. Design of a conductive fabric network by the sheet resistance method. *Text Res J* 2011; 81: 1568–1577.

22. Li L, Au WM, Ding F, et al. Wearable electronic design: electrothermal properties of conductive knitted fabrics. *Text Res J* 2014; 84: 477–487.

23. Tong JH, Ding F, Tao XM, et al. Temperature effect on the conductivity of knitted fabrics embedded with conducting yarns. *Text Res J* 2014; 84: 1849–1857.

24. Li L, Au WM, Li Y, et al. A novel design method for an intelligent clothing based on garment design and knitting technology. *Text Res J* 2009; 79: 1670–1679.

25. Zhao YF, Tong JH, Yang CX, et al. A simulation model of electrical resistance applied in designing conductive woven fabrics. *Text Res J* 2016; 86: 1688–1700.

26. Zhao YF, Li L. A simulation model of electrical resistance applied in designing conductive woven fabrics—Part II: fast estimated model. *Text Res J* 2018; 88: 1308–1318.